Penetration of Polyelectrolytes into Charged Poly (*N*-isopropylacrylamide) Microgel Layers Confined Between Two Surfaces

Molla R. Islam and Michael J. Serpe*

Department of Chemistry, University of Alberta, Edmonton, AB, T6G 2G2 (Canada)
E-mail: michael.serpe@ualberta.ca

Abstract:

PH and temperature sensitive poly (*N*-isopropylacrylamide) (pNIPAm) microgel-based etalons were fabricated by sandwiching a "monolithic" microgel layer between two semi-transparent, 15 nm Au layers. The devices exhibit visual color and multipeak reflectance spectra, both of which primarily depend on the distance between the Au surfaces (mediated by the microgel diameter). In this submission, we fabricate etalons from either pNIPAm-co-acrylic acid (pNIPAm-co-AAc) or pNIPAm-co-N-(3-Aminopropyl)methacrylamide hydrochloride (pNIPAm-co-APMAH) microgels and investigate their response to the presence of polycations or polyanions. We show that when the etalon is at a pH that renders the microgels multiply charged, the microgel layer of the etalon deswells in the presence of the oppositely charged polyelectrolyte; it is unresponsive to the presence of the like charged polyelectrolyte. Furthermore, the etalon's response depended on the thickness of the Au overlayer. For example, low molecular weight (MW) polyelectrolyte could penetrate all Au overlayer thicknesses; while high MW polyelectrolytes could only penetrate the etalons fabricated from thin Au overlayers. We hypothesize that this is due to a decrease in the Au pore size with increasing thickness, which excludes the high MW polyelectrolytes from penetrating the microgel-based layer. These devices show promise as MW selective sensors and biosensors.

Introduction:

Nature's apparent ease of controlling very complex biological processes has inspired researchers for years. This attempt at mimicry has led to a number of very important advances, in a variety of fields; most important to this submission are the advances in materials science. One outcome of this curiosity has been the development of responsive polymer-based materials.[1-4] Responsive polymers and materials can be simply defined as materials that can respond chemically or physically to the application of a stimulus.[5-7] Responsive polymer-based nanoparticles, microparticles, and composite materials are also well-known.[8-11] The most common stimuli responsive polymers developed thus far include those responsive to pH, temperature, ionic strength, concentration, light and magnetic field.[12-14] Other stimuli responsive systems have been studied and show potential for new applications.[15-20]

Poly (*N*-isopropylacrylamide) (pNIPAm) has by far been the most extensively studied responsive polymer to date. [21-31] PNIPAm is fully water-soluble and undergoes a volume phase transition from water solvated (swollen) to desolvated (collapsed) at pNIPAm's lower critical solution temperature (LCST) of ~32 °C. That is, at T > 32 °C the polymer takes on a globule conformation, while it is in a random coil conformation at T < 32 °C. PNIPAm-based colloids (nanogels or microgels, depending on their diameter) have also been synthesized, and are fully water swollen (large diameter) at T < 32 °C, while they are dehydrated (small diameter) at T > 32 °C.[7,11,17]

PNIPAm-based microgels can be readily synthesized via free radical precipitation polymerization. This approach is quite versatile, and can be used to yield nanogels/microgels with diameters ranging from 50 nm to 2 μm.[32-34] This synthetic approach is also very versatile in terms of the functionality that can be added to the microgel by simply adding functional

monomers to the reaction flask prior to initiation. A variety of functional microgels have been synthesized using this approach.[11,32,33,35,36] The most common comonomer is acrylic acid (AAc), [37,38] which is particularly interesting because it imparts pH responsivity to the pNIPAm-based microgels. AAc has a pK_a of ~4.25, therefore at pH > 4.25 the microgels are deprotonated and negatively charged, while they are neutral at pH < 4.25. Therefore, at high pH the microgels swell due to the charge-charge (Coulombic) repulsion in the polymer network. Furthermore, the Coulombic repulsion in the polymer network prevents the pNIPAm-based microgels from deswelling at elevated temperature.[32,39,40] Another advantage of AAc is its ability to react with other functional small molecules to add further responsivity, and/or functionality to the microgels.[41-44] Finally, the negative charges in the microgels as a result of their deprotonation can be exploited to study other fundamental properties of microgels, as was recently shown by Richtering and coworkers.[45] They showed that the LCST and diameter of poly-*N*-isopropylacrylamide-co-methacrylic acid (pNIPAM-co-MAA) microgels change with the introduction of charged polymers (polyelectrolytes) of opposite charge and depends on the distribution of polyelectrolytes in the microgels.

Recently, we reported on the fabrication of pNIPAm microgel-based optical devices. Figure 1 shows the basic structure of the devices, which are fabricated by "painting" a layer of pNIPAm-based microgels onto a 15 nm Au layer deposited onto a glass coverslip.[46] Another layer of Au is deposited onto the microgel layer to form a cavity defined by the microgel layer. These devices, which resemble traditional Fabry-Perot etalons (or simply etalons), exhibit visual color and distinct multipeak spectra.[47-49] A representative spectrum from a microgel-based etalon can be seen in Figure 1(b). The position of the peaks in the multipeak spectra (λ) can be predicted from equation 1,

$$\lambda = 2nd \cos \theta/m \quad \ldots \ldots \ldots (1)$$

where n is the refractive index of the dielectric layer, d is the mirror-mirror distance, θ is the angle of incident light relative to the normal, and m (an integer), is the order of the reflected peak.[50,51]

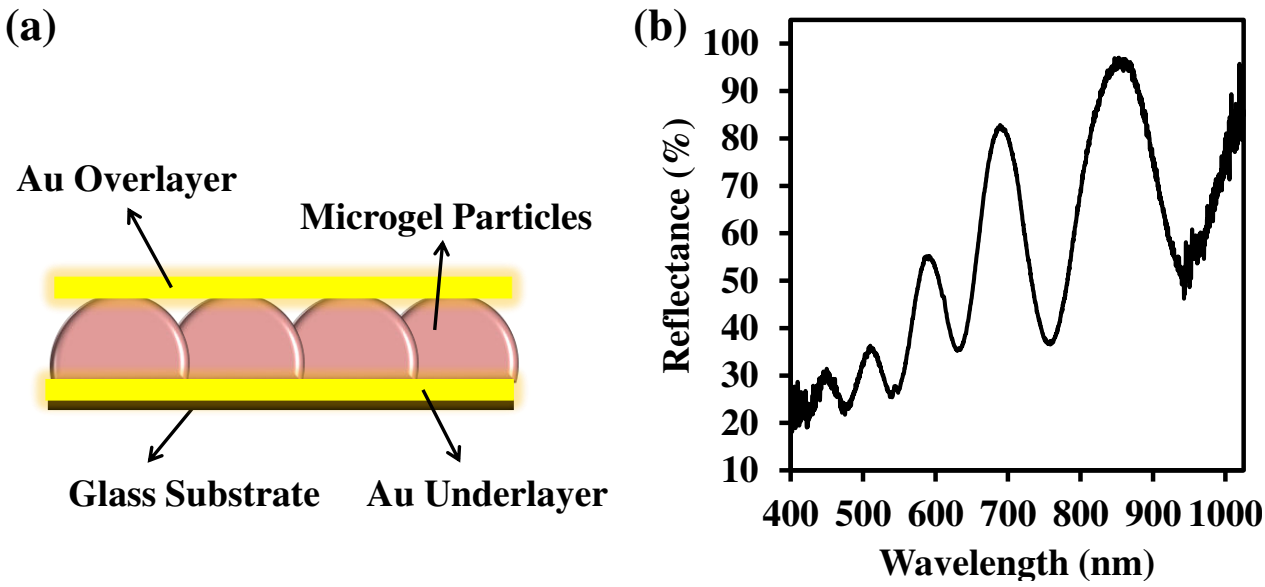

Figure 1: a) The basic structure of a microgel-based etalon. The Au overlayer in the figure is drawn as a planar layer, but is actually conformal to the microgel layer. b) Characteristic reflectance spectrum from a pNIPAm-co-AAc microgel-based etalon in water.

Due to the thermoresponsivity of the pNIPAm-based microgels, the color of the device, and the position of the peaks in the reflectance spectra, depends on the temperature of the solution they are immersed in. This is a direct result of the temperature dependent diameter of the pNIPAm-based microgels mediating the mirror-mirror distance (d in equation 1). In a recent effort to develop biosensors our group reported that aminophenylboronic acid (APBA)-functionalized pNIPAm-co-AAc microgels in an etalon respond to 3 mg/mL glucose by

exhibiting a red shift of the peaks in their reflectance spectra and a corresponding color change that could be detected visually.[52] This is a result of charge generation in the microgel layer as a result of glucose binding to the APBA groups, which leads to Coulombic repulsion in the microgel network and a concomitant swelling of the layer.

In this submission we exploit the microgel-diameter dependent optical properties of the pNIPAm-co-AAc microgel-based etalons to study the penetration of polyelectrolytes into the microgel based layers. As Richtering has shown, multiply charged microgels change their diameter in the presence of polyelectrolytes of the opposite charge.[45] Therefore, if a microgel-based etalon is in a solution of a pH that renders the microgels charged, it will change its optical properties in the presence of oppositely charged polyelectrolyte if the overlayer thickness (or the polymer molecular weight) is porous enough (or small enough) to allow the interaction.

Experimental:

Materials: N-Isopropylacrylamide was purchased from TCI (Portland, Oregon) and purified by recrystallization from hexanes (ACS reagent grade, EMD, Gibbstown, NJ) prior to use. N, N-methylenebisacrylamide (BIS) (99%), acrylic acid (AAc) (99%), and ammonium persulfate (APS) (98+ %) were obtained from Sigma-Aldrich (Oakville, Ontario) and were used as received. Poly (dimethylammonium chloride) solution (pDADMAC, MW 8,500, 28% in water) and N-(3-Aminopropyl)methacrylamide hydrochloride (APMAH) were purchased from Polysciences, Inc (Warrington, PA). PDADMAC solutions of MW <100,000 (35% in water); and MW 100,000-200,000 (20% in water); as well as poly (sodium 4- styrene-sulfonate), (PSS, MW 70,000) were purchased from Sigma-Aldrich (St. Louis, MO). Sodium chloride was obtained from EMD (Millipore, Billerica, MA) and deionized (DI) water with a resistivity of

18.2 MΩ•cm was used. Cr/Au annealing was done in a Thermolyne muffle furnace from Thermo Fisher Scientific (Ottawa, Ontario). Anhydrous ethanol was obtained from Commercial Alcohols (Brampton, Ontario). Sodium hydroxide (NaOH, 99.8%) and hydrochloric acid were purchased from Caledon Chemicals (Georgetown, Ontario) and were used as received. Fisher's finest glass coverslips were 25×25 mm and obtained from Fisher Scientific (Ottawa, Ontario). Cr was 99.999% and obtained from ESPI as flakes (Ashland, OR), while Au was 99.99% and obtained from MRCS Canada as shot (Edmonton, AB).

Microgel Synthesis:

Microgels composed of poly (*N*-isopropylacrylamide-co-acrylic acid) (pNIPAm-co-AAc) were synthesized via temperature-ramp, surfactant free, free radical precipitation polymerization as described previously.[34,47] The monomer mixture, with a total concentration of 154 mM, was comprised of 85% N-isopropylacrylamide (NIPAm) and 10% acrylic acid (AAc) with a 5% N,N'-methylenebisacrylamide (BIS) crosslinker. The monomer, NIPAm (17.0 mmol), and BIS (1.0 mmol) were dissolved in deionized water (100 mL) with stirring in a beaker. The mixture was filtered through a 0.2 μm filter affixed to a 20 mL syringe into a 200 mL 3-neck round-bottom flask. The beaker was rinsed with 25 mL of deionized water and then filtered into the NIPAm/BIS solution. The flask was then equipped with a temperature probe, a condenser and a N_2 gas inlet. The solution was bubbled with N_2 gas for ~1.5 h, while stirring at a rate of 450 rpm, allowing the temperature to reach 45 °C. AAc (2.0 mmol) was then added to the heated mixture with a micropipette in one aliquot. A 0.078 M aqueous solution of APS (5 mL) was delivered to the reaction flask with a transfer pipet to initiate the reaction. Immediately following initiation, a temperature ramp of 45 to 65 °C was applied to the solution at a rate of 30 °C/h. The reaction was allowed to proceed overnight at 65 °C. After polymerization, the reaction mixture was

allowed to cool down to room temperature and filtered through glass wool to remove any large aggregates. The coagulum was rinsed with deionized water and filtered. Aliquots of these microgels (12 mL) were centrifuged at a speed of ~8500 relative centrifugal force (rcf) at 23 °C for about 40 minutes to produce a pellet at the bottom of the centrifuge tube. The supernatant was removed from the pellet of microgels, which was then resuspended to the original volume (12 mL) using deionized water. This process was continued to a total of six times to remove any unreacted monomer and/or linear polymer from the microgel solution.

The same protocol as above was used to synthesize poly (*N*-isopropylacrylamide-co-N-(3-Aminopropyl)methacrylamide hydrochloride (pNIPAm-co-APMAH) microgels. These microgels were composed of NIPAm (90%), BIS (5%) and APMAH (5%).

Etalon Fabrication:

The details of the "painting" technique used to fabricate microgel-based etalons for these experiments has been reported elsewhere.[49] Briefly, 25 × 25 mm pre-cleaned glass coverslips were rinsed with DI water and ethanol and dried with N_2 gas, and 2 nm of Cr followed by 15 nm of Au were thermally evaporated onto them at a rate of ~0.2 Å s^{-1} and ~0.1 Å s^{-1}, respectively, using a Torr International Inc. model THEUPG thermal evaporation system (New Windsor, NY). The Cr acts as adhesion layer to hold the Au layer on the glass. The Au coated substrates were annealed at 250 °C for 3 h and then cooled to room temperature prior to use. An aliquot of about 12 mL of previously purified microgel solution was centrifuged for 30 min at 23 °C at ~8500 relative centrifugal force (rcf) to pack the microgels into a pellet at the bottom of the tube. After removal of the supernatant solution, the microgel pellet was vortexed and placed onto a hot plate at 30 °C. A previously coated Cr/Au substrate was rinsed with ethanol, dried with N_2, and then placed onto hot plate (Corning, NY) set to 30 °C. A 40 μL aliquot of the concentrated microgels

was put onto the substrate and then spread toward each edge using the side of a micropipette tip. The film was rotated 90°, and the microgel solution was spread again. The spreading and rotation continued until the microgel solution became too viscous to spread due to drying. The microgel solution was allowed to dry completely on the substrate for 2 h with the hot plate temperature set to 35 °C. After 2 h, the dry film was rinsed copiously with DI water to remove any excess microgels not bound directly to the Au. The film was then placed into a DI water bath and allowed to incubate overnight on a hot plate set to ~30 °C. Following this step, the substrate was again rinsed with DI water to further remove any microgels not bound directly to the Au substrate surface. Following this rinsing step, the film was dried with N_2 gas and placed into the metal evaporator, and an additional 2 nm Cr followed by Au layer of different thickness (5 nm, 15 nm, 25 nm and 35 nm) was deposited onto the microgel layer. The Au layer on top of the microgels is referred to as the Au overlayer. Following Au overlayer deposition, the device was soaked in DI water overnight on a hot plate at 30 °C and rinsed with DI water and dried with N_2 and subsequently used for experiments.

Reflectance Spectroscopy:

Reflectance measurements were conducted in a specially designed sample holder, which allowed for careful sample positioning, sample stability, sample injection, and temperature control. Reflectance spectra were collected using a USB2000+ spectrophotometer, a HL-2000-FHSA tungsten light source, and a R400-7-VIS-NIR optical fiber reflectance probe all from Ocean Optics (Dunedin, FL). The spectra were recorded using Ocean Optics Spectra Suite Spectroscopy Software over a wavelength range of 350-1025 nm.

Polyelectrolyte Penetration Experiment:

In this submission, we were interested in understanding how Au overlayer thickness affected the accessibility of the etalon's microgel layer to species of varying molecular weights. Therefore, to be sure that the interactions were solely a result of penetration of the polyelectrolyte through the Au overlayer, the sides of the etalon were sealed with clear nail polish. We have shown that this sealing protocol is sufficient to guarantee microgel accessibility through the Au overlayer only (data not shown). After sealing, the etalons were dried at ambient temperature overnight and subsequently soaked in pH 6.5 solution (ionic strength 2 mM adjusted with NaCl) for subsequent use. For the experiments, the etalon was transferred to a specially designed sample chamber filled with 30 mL of pH 6.5 solution and the temperature of the chamber was set to 25 °C. The light source's intensity was adjusted to yield an optimal reflectance spectrum, similar to Figure 1(b). The polyelectrolyte solutions (either pDADMAC or PSS) were prepared in a pH 6.5 solution and the pH of the resulting solutions was adjusted to 6.5 by adding drops of 0.1 M or 0.01 M NaOH solutions. Successive additions of fixed volumes of polyelectrolyte solutions to the chamber were made after the etalon's spectrum was stable for at least 60 min. On average, 2 h was needed for stabilization. During the addition of polyelectrolyte solutions to the chamber the pH of the resultant solution was monitored using a pH meter and adjusted to pH 6.5 with 0.1 M NaOH solution if necessary. It was confirmed that the pH of the system was 6.5 throughout each experiment.

RESULTS AND DISCUSSION:

One of the most important processes in biological system is the translocation of biological entities (DNA, protein, etc) through membrane channels or pores of cells. Understanding the process is crucial to develop various methods for nano-biotechnology related

to DNA, bacterial phage translocation and drug delivery. There has been a number of theoretical and simulation studies to unveil the physics of macromolecular translocation through pores or membranes.[53-60] In a similar effort to study the penetration of charged polymers through a porous layer to influence the solvation state and hence the diameter of charged microgel we studied the penetration of pDADMAC and PSS (Scheme 1) into the confined microgel layer of an etalon. In addition to using this as a platform to study fundamental aspects of polyelectrolyte penetration through pores, we are also interested in this behavior to further use the phenomenon for etalon-based sensing.

Scheme 1: Chemical formula of pDADMAC and PSS.

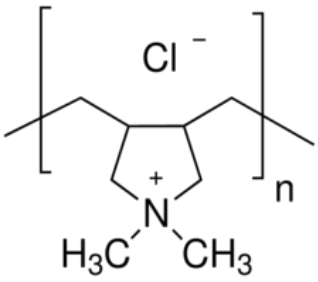

pDADMAC

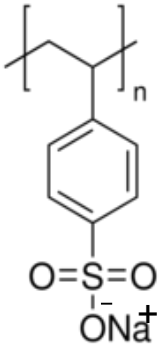

PSS

As we mention above, Richtering and coworkers, [45] showed that charged pNIPAm-based microgels change diameter in the presence of charged polymer (polyelectrolyte) of opposite charge. In this submission we take advantage of this phenomenon to determine how polyelectrolyes of differing molecular weights (MW) interact with the microgel layer between the etalon's two Au layers. In a previous study we, and others, have shown that the average pore

size decreases with increasing Au overlayer thickness. [49] We want to make clear that the pores are not uniform with respect to size, shape and geometry. There can be big and small pores of various geometries, as well as defects in each overlayer, but the "average pore size" decreases with Au overlayer thickness.[49, 61-63] the Au porosity decreases with increasing Au overlayer thickness.[49] Therefore, if the Au overlayer thickness results in a pore size that allows a polymer of a given MW into the microgel layer, an optical response should be observed due to the microgel diameter decrease as a function of polyelectrolyte mediated intramolecular crosslinking in the microgels of the layer. The process is depicted schematically in Figure 2. This is important to understand to use these devices as sensors for large molecular weight biological species, e.g., protein and DNA.

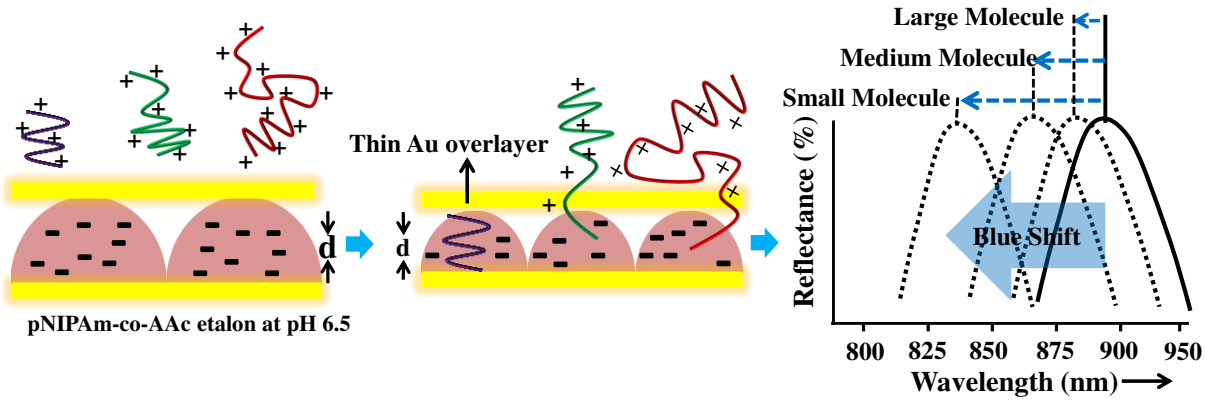

Figure 2: Polyelectrolyte penetration through the porous Au overlayer of an etalon.

Initial experiments were performed on etalons composed of pNIPAm-co-AAc microgels. It is well known that AAc modified microgels exhibit pH responsivity. That is, at pH > pK_a for AAc (~4.25) the microgel network becomes negatively charged and the microgels swell due to Coulombic repulsion. At a pH < pK_a, the AAc groups in the microgels are protonated, and hence the microgels are neutral. The resultant pH response of pNIPAm-co-AAc microgels immobilized

in an etalon is shown in Figure 3. As can be seen, the observed reflectance peak from an etalon in a solution of a pH of 6.5 is higher in wavelength compared to its position in pH 3.0 solution. This is due to the charges generated from AAc deprotonation in the microgel layer of the etalon causing the microgels to swell due to Coulombic repulsion. When the solution pH is brought back to pH 3.0, the observed reflectance peak shifts to its initial position as shown in Figure 3.

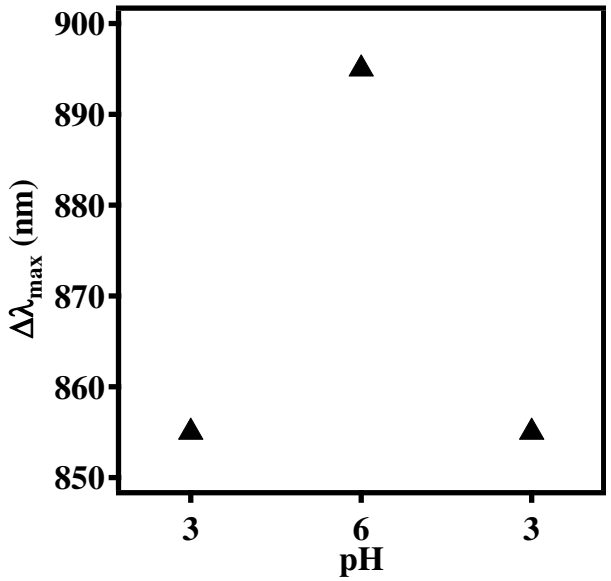

Figure 3: The effect of solution pH on the λ_{max} of reflectance spectra of pNIPAm-co-AAc etalon.

Since it was determined that multiple charges on pNIPAm-co-AAc microgels could be formed at pH 6.5, we then exposed them to solutions of the positively charged polymer (polycation), pDADMAC. The solutions had a concentration of 0.1 M monomer and pH of 6.5. Regardless, the pH of the solution was continuously monitored with a pH meter. Figure 4(a) shows that λ_{max} shifted to lower wavelength upon addition of pDADMAC confirming the penetration of pDADMAC into the microgel layer. Also, as can be seen in lower panel of Figure 4(a), there is no significant shift in the peak position when pDADMAC is added to the etalon at

pH 3.0. This observation proves that the response is likely electrostatic in nature, as observed by Richtering.[45]

Furthermore, we investigated whether the anionic microgel layer (i.e., etalon in pH 6.5 solution) could interact with a polyanion. To investigate this, we added a solution of 0.1 M monomer PSS to the pNIPAm-co-AAc in pH 6.5 solution. As can be seen in Figure 4 (b), no significant shift in the peak position was observed. Additionally, as can be seen in Figure 4(b), no change in peak position was observed when PSS solution was added to the pNIPAm-co-AAc microgel-based etalon in pH 3.0 solution. Finally, as shown in Figure 5, pNIPAm microgel-based etalons (i.e., microgels with no AAc) did not show any significant response to the addition of pDADMAC or PSS.

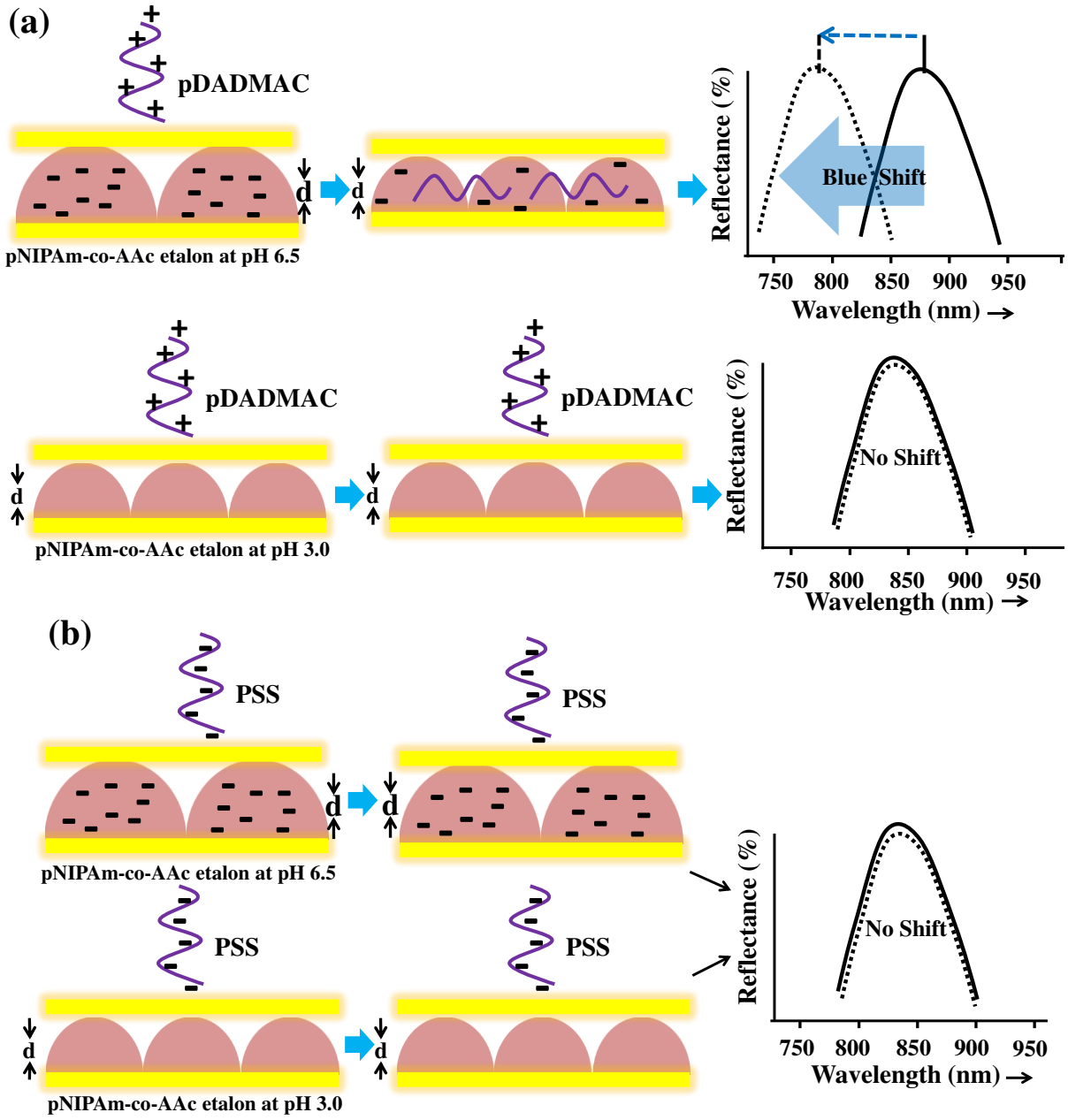

Figure 4: (a) Interaction of pDADMAC with pNIPAm-co-AAc microgel-based etalons in pH 6.5 and pH 3.0 solution. b) Interaction of PSS with pNIPAm-co-AAc microgel-based etalons in pH 6.5 and pH 3.0 solution.

We further sythesized pNIPAm-co-APMAH microgels, which are polycationic at pH < ~10. The etalons were stabilized in pH 6.5 solution, and showed a blue shift in the peak position

upon addition of PSS, as can be seen in Figure 6. As expected from our experiments above, there was no significant spectral shift upon addition of pDADMAC.

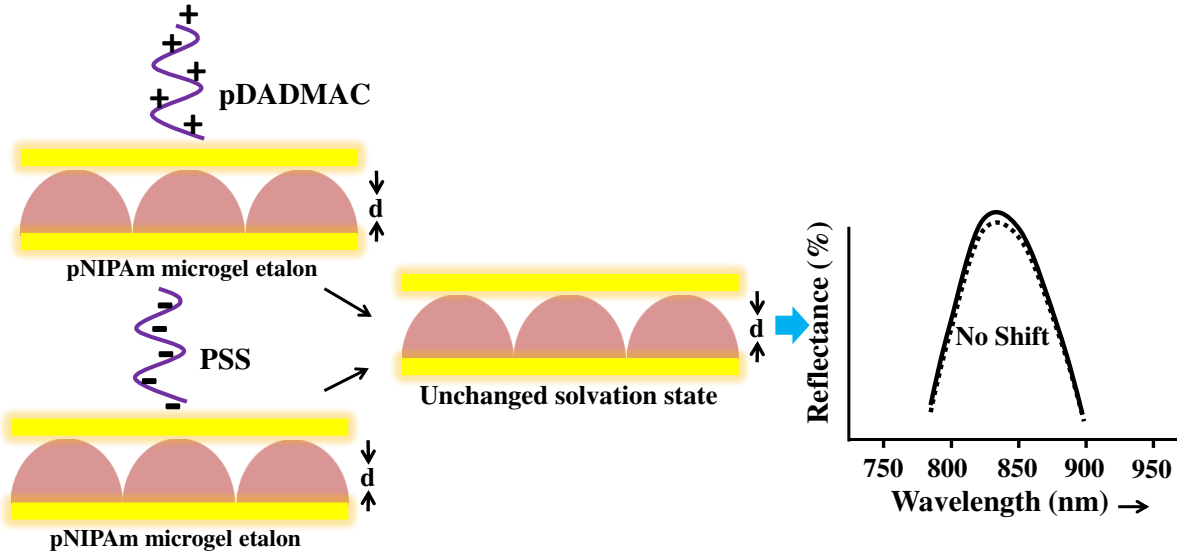

Figure 5: PNIPAm- based microgel (No AAc) etalon's interaction with pDADMAC and PSS.

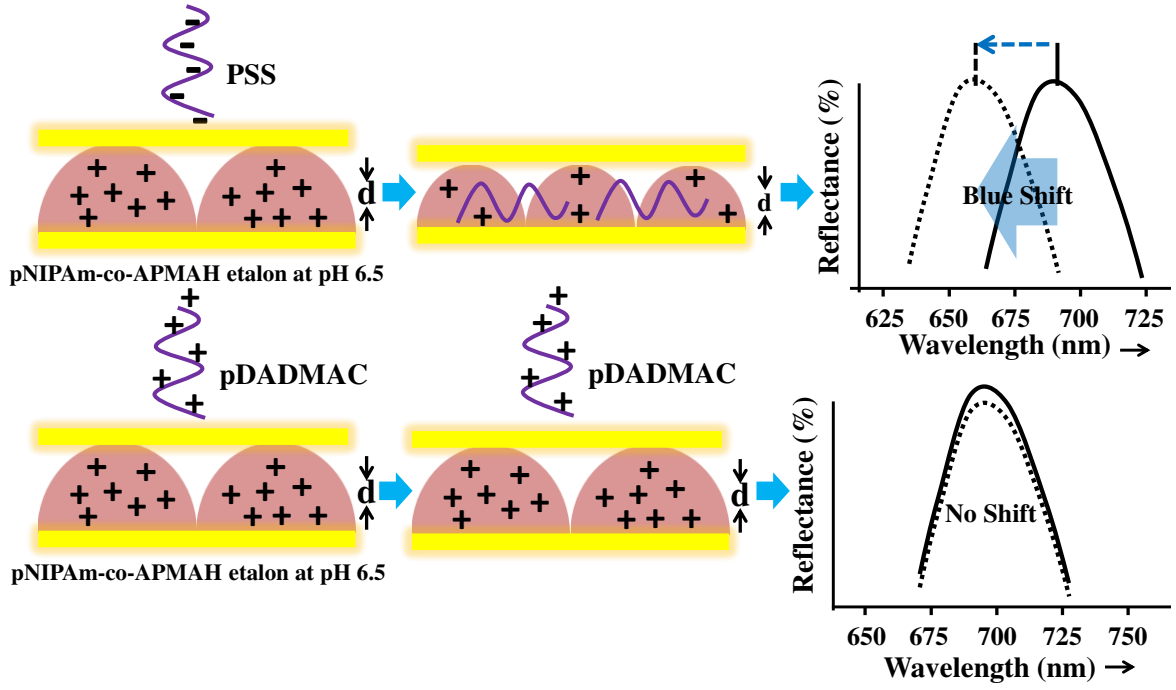

Figure 6: Interaction of pDADMAC and PSS with PNIPAm-co-APMAH etalon at 6.5.

Effect of Overlayer Thickness and Polyelectrolyte MW:

Figure 7 shows how the Au overlayer thickness affected the penetration of polyelectrolytes into the etalon's microgel layer. Furthermore, Figure 7 shows how the etalon's response depends on polyelectrolyte MW. To conduct these experiments, an etalon composed of a given overlayer thickness was stabilized in pH 6.5 solution, and a given amount of pDADMAC was added. The total shift ($\Delta\lambda_{max}$) of one of the etalons reflectance peaks was calculated and plotted. It is important to note that peaks with the same order (m) were compared for this study. As can be seen in Figure 7(a), low MW pDADMAC (MW=8500) results in a blue shift of 70 nm when the overlayer thickness was 5 nm. This is the largest shift observed for all the experiments. For the same MW pDADMAC, the response is decreased to 35 nm when the Au overlayer thickness is increased to 15 nm. As can be seen, the response continuously diminishes as the overlayer thickness increases further. From the data, we conclude that pDADMAC can penetrate into the microgel layer as long as the pore diameter is large enough to allow the pDADMAC to penetrate the microgel layer. Another possibility is that the Au overlayer becomes so thick that the pDADMAC cannot feel the negative charge in the microgel layer. While this is possible, it is not likely since the osmotic pressure differences should drive the pDADMAC into the microgel layer.

To investigate this further, other etalons were fabricated with various Au overlayer thicknesses, and their response to pDADMAC of various MW was characterized. The etalon's were likewise stabilized in pH 6.5 solution and exposed to pDADMAC solutions with weight average MW of < 100,000, and 100,000-200,000. As can be seen from Figure 7(b) and 7(c) the response at all overlayer thicknesses was greater for the 100,000 MW compared to the higher MW pDADMAC. Furthermore, these responses are significantly lower when compared to the low MW pDADMAC. The same phenomenon was observed for etalons composed of pNIPAM-

co-APMAH microgels. As seen in Figure 8, the response depended dramatically on the Au overlayer thickness.

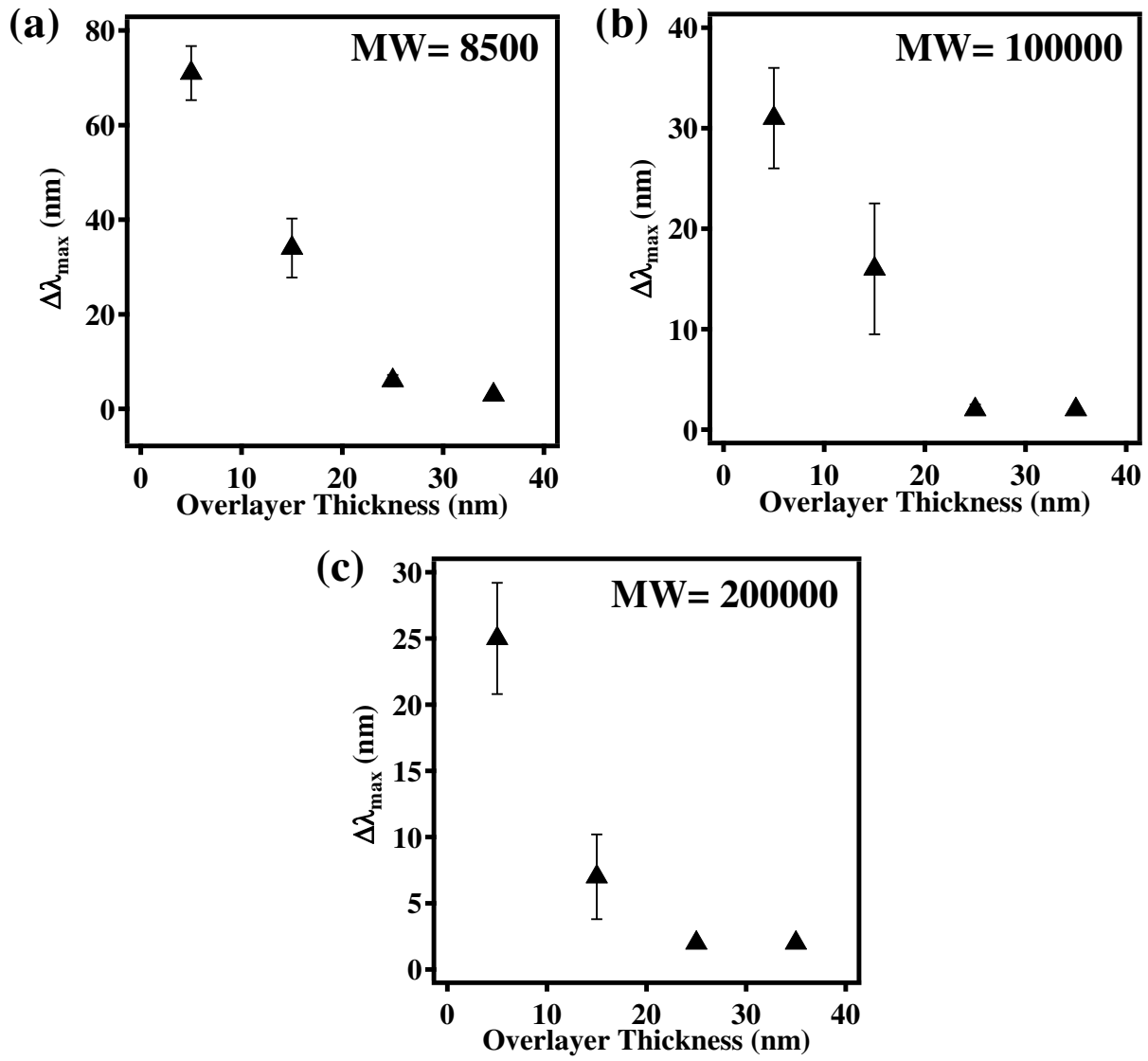

Figure 7: Shift of λ_{max} for pNIPAm-co-AAc etalons in pH 6.5 after addition of pDADMAC solution with MW a) 8500, b) <100,000 and c) 100,000-200,000.

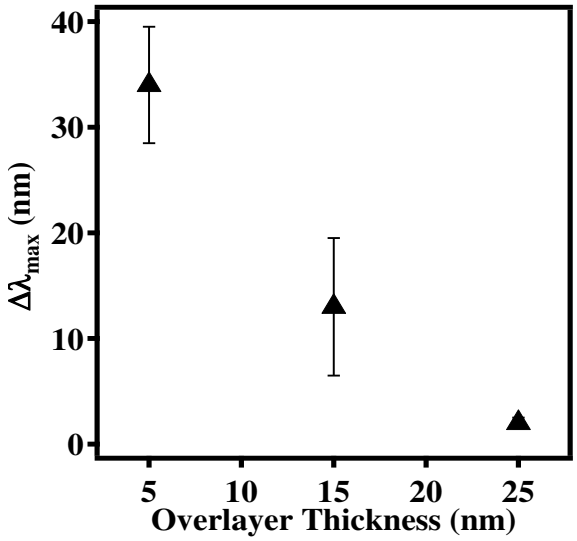

Figure 8: Shift of λ_{max} of pNIPAm-co-APMAH etalon on addition of PSS with overlayer thickness.

Comparison to Existing Results:

In previous studies, Muthukumar et al.[58] showed that low molecular weight polymers are able to penetrate nanopores more effectively than high MW polymers. In our studies, we found the same phenomenon. Specifically, when the Au overlayer pore size was decreased (by increasing the Au overlayer thickness) only low MW polyelectrolytes could effectively penetrate into the microgel layer. In our system, the only forces facilitating the interactions are electrostatic, while other studies looked at polyelectrolyte penetration through pores under chemical potential gradient, [57] solvent flow, [59] and applied electric field.[58,60] In our system, we can consider the Au overlayer as a porous membrane with a discontinuous porous network which needs to be "navigated" by the polyelectrolytes of different MW to enter the microgel layer. It has been shown by several groups that short (low MW) polymer chains translocate through pores faster (and more effectively) than long (high MW) polymer chains for a given pore length. The translocation is controlled by the competition between entropic (reduced configurational freedom due to narrow channel confinement during translocation) and hydrodynamic effects (polymer

elongation due to coil-stretch transition in the pore region) based on what critical penetration length (depends on polymer length) is required for successful penetration for the chain.[53-60] Due to the polymer elongation, the entropic barrier of the translocation is reduced. As a result, one end of polymer can penetrate and achieve the critical penetration length and translocate through the pores.[54] In our system, the pore network is different than one continuous pore, with a defined length; our pores are not necessarily continuous and have a variety of diameters and lengths. We hypothesize that hydrodynamic contribution from chain elongation over entropic barrier is not enough in our system to overcome the barrier of discontinuity of pore network. As a result, the medium/large polyelectrolyte chains cannot penetrate through the Au overlayer fully over a finite time and only a partial complexation with the microgel is possible. For small chains, the critical penetration length is smaller and achieved faster while for long polymers, the critical penetration length is large. Therefore, we hypothesize that small polymers translocate faster with all thickness while for long polymer cannot penetrate completely to interact with microgel.

Conclusion:

In this submission, we showed that polyelectrolytes can penetrate Au overlayers of etalons. The penetration of the polyelectrolytes into the microgel layer of the etalons is detected as a shift in the peaks of the reflectance spectra. Through the proper controls, we were able to conclude that the response is a result of polyelectrolyte mediated intramolecular crosslinking of the microgels that make up the etalons. We finally showed that the response of the etalon to the introduction of polyelectrolyte depended critically on Au overlayer thickness and polyelectrolyte MW. Specifically, if the polyelectrolyte's MW is of small enough to penetrate the pores of the

etalon, they will enter the microgel layer and cause a response if the polyelectrolyte is opposite in charge compared to the microgels. This study shows the potential of using microgel-based etalons as a tool for biosensing and detection of polyelectrolyte with different MWs.

Acknowledgements:

MJS acknowledges funding from the University of Alberta (the Department of Chemistry and the Faculty of Science), the Natural Science and Engineering Research Council (NSERC), the Canada Foundation for Innovation (CFI), the Alberta Advanced Education & Technology Small Equipment Grants Program (AET/SEGP) and Grand Challenges Canada. MJS acknowledges Mark McDermott for the use of the thermal evaporator.

References:

(1) Lee, H.; Lee, B. P.; Messersmith, P.B. *Nature* **2007**, *448*, 338-342.

(2) Lee, H.; Dellatore, S. M.; Miller, W. M.; Messersmith, P. B. *Science* **2007**, *318*, 426-430.

(3) Haller, C. M.; Buerzle, W.; Brubaker, C.E.; Messersmith, P. B.; Mazza, E.; Ochsenbein-Koelble, N.; Zimmermann, R.; Ehrbar, M. *Prenatal Diagnosis* **2011**, *31*, 654-660.

(4) Capadona, J.R.; Shanmuganathan, K.; Tyler, D. J.; Rowan, S. J.; Weder, C. *Science* **2008**, *319*, 1370-1374.

(5) Suzuki, A.; Tanaka, T. *Nature* **1990**, *346*, 345-347.

(6) Gutowska, A.; Bae, Y.H.; Jacobs, H.A.; Feijen, J.; Kim, S.W. *Macromolecules* **1994**, *27*, 4167-4175.

(7) Pelton, R. *Science* **2000**, *85*, 1-33.

(8) Kwon, I.C.; Bae, Y.H.; Kim, S.W. *Nature* **1991**, *354*, 291-293.

(9) Wang, T.; Liu, D.; Lian, C.; Zheng, S.; Liu, X.; Tong, Z. *Soft Matter* **2012**, *8*, 774-783.

(10) Haraguchi, K.; Murata, K.; Takehisa T. *Macromolecules* **2012**, *45*, 385-391.

(11) Gong, J. P. *Soft Matter* **2010**, *6*, 2583-2590.

(12) Ayano, E.; Karaki, M.; Ishihara, T.; Kanazawa, H.; Okano, T. *Colloids Surf. B* **2012**, *99*, 67-73.

(13) Nash, M.A.; Waitumbi, J.N.; Hoffman, A.S.; Yager, P.; Stayton, P.S. *ACS Nano* **2012**, *6*, 6776-6785.

(14) Thomas, C.S.; Xu, L.; Olsen, B.D. *Biomacromolecules* **2012**, *13*, 2781-2792.

(15) Black, A. L.; Lenhardt, J. M.; Craig, S. L. *J. Mater. Chem*. **2011**, *21*, 1655-1663.

(16) Brochu, A. W.; Craig, S. L.; Reichert, W. M. *J. Biomed. Mater. Res. Part A* **2011**, 96A, 492-506.

(17) Chen, Y.; Spiering, A. J. H.; Karthikeyan, S.; Peters, G. W. M.; Meijer, E. W.; Sijbesma, R. P. *Nat. Chem.* **2012**, *4*, 559-562.

(18) Craig, S. L. *Nature* **2012**, *487*, 176-177.

(19) Meijer, E. W.; Nijhuis, S.; Havinga, E. E. *Philips J. Res.* **1988**, *43*, 506-530.

(20) Ma, Y.; Dong, W.-F.; Hempenius, M.A.; Möhwald H.; Vancso, G.J. *Nature Materials* **2006**, 5, 724-729.

(21) Hoffmann, M.; Siebenbürger, M.; Harnau, L.; Hund, M.; Hanske, C.; Lu, Y.; Wagner, C. S.; Drechsler, M.; Ballauff, M. *Soft Matter* **2010**, *6*, 1125-1128.

(22) Wu, C.; Zhou, S. *Macromolecules* **1995**, *28*, 8381-8387.

(23) Kawaguchi, H.; Fujimoto, K.; Mizuhara, Y. *Colloid Polym. Sci.* **1992**, *270*, 53-57.

(24) Zhang, G.; Wu, C. *J. Am. Chem. Soc.* **2001**, 123, 1376-1380.

(25) Debord, J.D.; Lyon, L.A. *Langmuir* **2003**, *19*, 7662-7664.

(26) Hoare T.; Pelton, R. *Macromolecules* **2007**, *40*, 670-678.

(27) Kleinen, J.; Richtering, W. *J. Phys. Chem. B* **201**1, *115*, 3804-3810.

(28) Wu, C.; Wang, X. *Phys. Rev. Lett.* **1998**, *80*, 4092-4094.

(29) Ali, M.M.; Aguirre, S.D.; Xu, Y.; Filipe, C.D.M.; Pelton, R.; Li, Y. *Chem. Commun.* **2009**, *43*, 6640-6642.

(30) Serpe, M.J.; Lyon, L.A. *Chem. Mater.* **2004**, *16*, 4373-4380.

(31) Su, S.; Ali, M.M.; Filipe, C.D.M.; Li, Y.; Pelton, R. *Biomacromolecules* **2008**, *9*, 935-941.

(32) Serpe, M. J.; Jones, C. D.; Lyon, L. A. *Langmuir* **2003**, 19, 8759-8764.

(33) Gan, D. J.; Lyon, L. A. *Macromolecules* **2002**, *35*, 9634-9639.

(34) Meng, Z. Y.; Cho, J. K.; Debord, S.; Breedveld, V.; Lyon, L. A. *J. Phys. Chem. B* **2007**, *111*, 6992-6997.

(35) Kratz, K.; Hellweg, T.; Eimer, W. *Colloids Surf. A* **2000**, *170*, 137-149.

(36) Zhou, S.; Chu, B. *J. Phys. Chem. B* **1998**, *102*, 1364-1371.

(37) Burmistrova, A.; von Klitzing, R. *J. Mater. Chem.* **2010**, *20*, 3502-3507.

(38) Jones C.D.; Lyon, L.A. *Macromolecules* **2000**, *33*, 8301-8306.

(39) Bromberg, L.; Temchenko, M.; Hatton, T.A. *Langmuir* **2000**, *18*, 4944-4952.

(40) Morris, G.E.; Vincent, B.; Snowden, M.J. *J Colloid Interface Sci.* **1997**, *190*, 198-205.

(41) Meng, Z.; Hendrickson, G. R.; Lyon, L. A. *Macromolecules* **2009**, *42*, 7664-7669 .

(42) Zhou, S.; Chu, B. *J. Phys. Chem. B* **1998**, *102*, 1364-1371.

(43) Nayak, S.; Lee, H.; Chmielewski, J.; Lyon, L. A. *J. Am. Chem. Soc.* **2004**, *126*, 10258-10259.

(44) Schmidt, S.; Hellweg, T.; von Klitzing, R. *Langmuir* **2008**, *24*, 12595-12602.

(45) Kleinen, J.; Richtering, W. *Colloid Polym. Sci.* **2011**, *289*, 739-749.

(46) Sorrell, C.D.; Carter, M.C.D.; Serpe, M.J. *ACS Appl. Mater. Interfaces*, **2011**, *3*, 1140-1147.

(47) Sorrell, C.D.; Carter, M.C.D.; Serpe, M.J. *Adv. Funct. Mater.* **2011**, *21*, 425-433.

(48) Sorrell, C.D.; Serpe, M.J. *Adv. Mater.* **2011**, *23*, 4088-4092.

(49) Carter, M.C.D.; Sorrell, C.D.; Serpe, M.J. *J. Phys. Chem. B* **2011**, *115*, 14359-14368.

(50) Brooker, G. *Modern Classical Optics;* Oxford University Press: Oxford, U.K., **2003**.

(51) Vaughan, J. M. *The Fabry-Perot Interferometer: History, Theory, Practice and Applications*; *Taylor & Francis Group*: New York, **1989**; pp 583.

(52) Sorrell, C.D.; Serpe, M.J. *Anal. Bioanal. Chem.* **2012**, *402*, 2385-2393.

(53) Wong, C. T. A.; Muthukumar, M. *J. Chem. Phys.* **2008**, *128*, 154903.

(54) Wong, C. T. A.; Muthukumar, M. *J. Chem. Phys.* **2007**,*126*, 164903.

(55) Kong, C.Y.; Muthukumar, M. *J. Chem. Phys.* **2004**, *120*, 3460-3466.

(56) Muthukumar, M. *J. Chem. Phys.* **2003**, *118*, 5174-5184.

(57) Muthukumar, M. *Electrophoresis* **2002**, *23*, 1417-1420.

(58) Murphy, R. J.; Muthukumar, M. *J. Chem. Phys.* **2007**, *126*, 051101.

(59) Ledesma-Aguilar, R.; Sakauebc, T.; Yeomans, J. M. *Soft Matter* **2012**, *8*, 1884-1992.

(60) Meller, A.; Nivon, L.; Branton, D. *Phys. Rev. Lett.* **2001**, *8*6, 3435-3438.

(61) Norrman, S.; Andersson, T.; Peto, G.; Somogyi, S. *Thin Solid Films* **1981**, *77*, 359-366.

(62) Golan, Y.; Margulis, L.; Rubinstein, I. *Surf. Sci.* **1992**, *264*, 312-326.

(63) Roland, T.; Khalil, A.; Tanenbaum, A.; Berguiga, L.; Delichère,P.; Bonneviot, L.; Elezgaray, J.; Arneodo, A.; Argoul, F. *Surf. Sci.* **2009**, *603*, 3307-3320.

For Table of Contents Only, Table of Contents Graphic:

Penetration of Polyelectrolytes into Charged Poly (*N*-isopropylacrylamide) Microgel Layers Confined Between Two Surfaces by Molla R. Islam and Michael J. Serpe*